

Scaling of local density correlations in a fluid close to freezing

F. Saija^{a)}

Istituto di Tecniche Spettroscopiche del CNR Via La Farina 237, I-98123, Messina, Italy

S. Prestipino and P. V. Giaquinta

Istituto Nazionale per la Fisica della Materia, Unità di Ricerca di Messina and Università degli Studi di Messina, Dipartimento di Fisica, Contrada Papardo, 98166 Messina, Italy

(Received 8 June 2001; accepted 6 August 2001)

We simulated the equilibrium properties of some reference model fluids, with hard-core, Yukawa and Lennard-Jones interactions, and compared their local density profiles in thermodynamic states where the residual multiparticle entropy (RMPE), an established and rather sensitive indicator of the incipient ordering of the fluid into a more structured phase, happens to vanish. We found that, once interparticle distances have been referred to the average separation between nearest-neighbor particles, the radial distribution functions (RDF) coalesce—from the second coordination shell onwards—onto nearly the same spatial profile. This property was ascertained for different model systems in different thermodynamic conditions but for the shared zero-RMPE constraint. The emergence of a scaling relation for the RDF's in the fluid phase further enlightens the nature of the structural condition that is singled out by the vanishing of the RMPE. © 2001 American Institute of Physics. [DOI: 10.1063/1.1406528]

I. INTRODUCTION

Recently, Saija and co-workers,¹ while investigating the ordering properties of hard-core and Lennard-Jones (LJ) particles in two dimensions (2D), highlighted the existence of a scaling relation for the radial distribution function (RDF) of both model fluids when the thermodynamic states that are being compared refer to a condition such that the excess entropy of the system can be exactly expressed as:

$$s_{(\text{ex})} = -\frac{1}{2}\rho \int \mathbf{dr} [g(r)\ln g(r) - g(r) + 1], \quad (1)$$

where ρ is the number density, $g(r)$ is the RDF and $s_{(\text{ex})}$ is the difference between the total entropy per particle of the fluid (measured in units of the Boltzmann constant k) and the corresponding noninteracting value. In general, the r.h.s. of Eq. (1) represents the contribution of two-body density correlations only to the excess entropy.² Correspondingly, Eq. (1) is tantamount to the vanishing of the re-summed contributions associated with correlations involving at least triads of particles.^{3,4}

$$\Delta s = s_{(\text{ex})} - s_2, \quad (2)$$

where s_2 is the pair entropy and Δs is the so-called residual multiparticle entropy (RMPE). The relevance of the condition $\Delta s = 0$ as a one-phase ordering criterion has been documented for a variety of thermodynamic phenomena both in continuous systems³⁻⁹ as well as in lattice fluids.^{10,11}

Hansen and Schiff, while studying the structural properties of fluids interacting through inverse-power repulsive potentials at crystallization, had already observed that the oscillations of the RDF beyond the first peak are similar in amplitude, in the two extreme cases of hard spheres and of a

Coulomb potential, although the positions are systematically shifted.¹² In this paper we aim to examine in closer and more critical detail the “collapse” of the RDF's of different three-dimensional (3D) fluids onto a common spatial profile, after density effects have been properly taken into account. In order to do this, we further extended the analysis performed in Ref. 1 to also include, besides hard spheres (HS) and LJ particles, hard-core Yukawa fluids (HCYF), i.e., hard spheres attracting each other through a Yukawa potential.

II. MODELS AND METHOD

We performed standard Metropolis Monte Carlo (MC) simulations of the following model potentials:

$$u_{\text{HS}}(r) = \begin{cases} +\infty & r < \sigma \\ 0 & r \geq \sigma \end{cases}, \quad (3)$$

$$u_{\text{HCYF}}(r) = \begin{cases} +\infty & r < \sigma \\ -\epsilon(\sigma/r)\exp[-z((r/\sigma)-1)] & r \geq \sigma \end{cases}, \quad (4)$$

$$u_{\text{LJ}}(r) = 4\epsilon \left[\left(\frac{\sigma}{r} \right)^{12} - \left(\frac{\sigma}{r} \right)^6 \right], \quad (5)$$

where r is the interparticle distance, σ is a geometrical scale factor (the sphere diameter for hard-core particles), and ϵ is the depth of the attractive well. The range of the Yukawa potential can be adjusted through the parameter z . In the following, we shall use reduced temperature units: $T^* = kT/\epsilon$.

The simulations were performed at constant temperature T in 3D. The number of particles in each sample, replicated with periodic boundary conditions, ranged between 800 and 1000. Each simulation run was started from a perfect face-centered-cubic (FCC) crystal configuration. The equilibration

^{a)}Electronic address: saija@me.cnr.it

of the samples typically took, depending on the density, $2 \times 10^5 - 1 \times 10^6$ MC sweeps, a sweep consisting of one attempt to sequentially change all particle positions. The maximum displacement of a particle was adjusted along the run so as to keep the acceptance ratio of the MC moves as close to 0.5 as possible. The relevant thermodynamic averages were computed over $4 \times 10^5 - 7 \times 10^5$ MC sweeps. The RDF histogram was constructed with a spatial resolution $\Delta r = \sigma/20$, and was updated every 100–500 MC sweeps. The RDF was computed up to a distance $R_{\max} = L/2$, where $L = (N/\rho)^{1/3}$ is the length of the simulation box. The RDF was never found to differ significantly from unity at a distance of order R_{\max} . The fulfillment of this condition is crucial for ensuring an accurate numerical estimate of the pair entropy at liquid densities.

III. THE SCALING CRITERION

According to the preliminary evidence presented in Ref. 1 for hard-core and LJ particles in 2D as well as 3D, the spatial profile of the RDF looks the same—as far as the phase and the amplitude of the oscillations beyond the second peak are concerned—for different systems and/or thermodynamic conditions, provided that (i) the states in which the RDF's are being compared are such that the RMPE of the fluid vanishes and (ii) the interparticle separation r is referred to the average distance l between nearest-neighbor (NN) particles:

$$g_{\alpha}(r_I) \approx g_{\beta}(r_{II}), \quad \text{if } \frac{r_I}{l_{\alpha}(I)} = \frac{r_{II}}{l_{\beta}(II)}, \quad (6)$$

where the subscripts α, β label the model systems that are currently being considered (i.e., HS, HCYF, LJ), while I and II identify two distinct thermodynamic conditions either for two different fluids or for the same fluid ($\alpha = \beta$) under the zero-RMPE constraint. The characteristic distance l_{α} can be estimated as $\rho_{\alpha}^{-1/3}$.¹ Equation (6) can then be rewritten as

$$g_{\alpha}(r) \approx g_{\beta}(\gamma r), \quad (7)$$

where

$$\gamma = \frac{l_{\beta}(II)}{l_{\alpha}(I)} = \left(\frac{\rho_{\alpha}}{\rho_{\beta}} \right)^{1/3}. \quad (8)$$

It is rather obvious that any “scaling relation” for the RDF like the one formalized in Eq. (6), cannot hold, in general, at very short distances where the influence of a specific potential on the detailed shape of the RDF is rather strong. This is particularly evident for potentials with a hard-core repulsion as compared to a soft one. Saija and co-workers observed that the agreement between the scaled RDF's was extremely good from about the second peak onwards.¹ The efficacy of the above r -scaling procedure in “according” the phases of the damped oscillations of the RDF's of different systems in different thermodynamic states at high enough values of the density may not look particularly surprising in that the NN separation is a “natural” reference distance for comparing spatial correlations in a way that is not *a priori* biased by easily predictable density (viz., packing) effects on the relative arrangement of particles in the fluid. What, to us, is

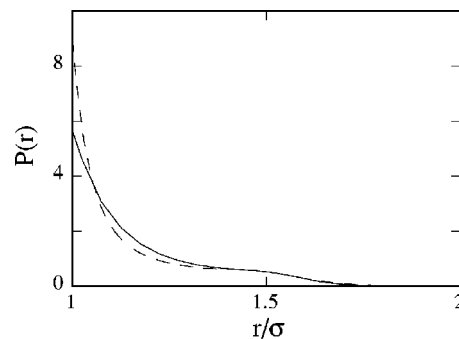


FIG. 1. Histogram of the Voronoi nearest-neighbor particles that are located at a distance r from a given reference particle for hard spheres (continuous line) and for a HCYF with $z=7$ (dashed line). Both fluids have the same density, $\rho\sigma^3 = 0.95$, the reduced temperature of the HCYF being $T^* = 0.5$.

definitely less obvious is that the amplitudes of the oscillations do substantially coincide (within the numerical accuracy of the calculation) when the condition $\Delta s(\rho, T) = 0$ is fulfilled. Before commenting further on this result, we shall check the assumption made on the mean NN separation in Ref. 1, where it was estimated as $\rho^{-1/3}$. The distance l , which obviously depends on the thermodynamic state of the fluid, can be unambiguously defined and calculated through the so-called Voronoi construction:¹³ the embedding space is first partitioned into polyhedral cells, each representing the set of points which are closer to a given particle than to any other particle. By construction, every face of a Voronoi cell lies halfway between two opposite (with respect to the face) neighboring particles and is orthogonal to the axis joining them. The number of faces of the Voronoi polyhedron enclosing a given reference particle is thus equal, by definition, to the number of its NN particles (n_{NN}). Hence, for any spatial configuration generated by the MC algorithm, one can identify the nearest neighbors of any particle in the fluid and, after performing an average over all the sampled configurations, construct the histogram $P(r)$ of the NN particles that are located at distance r from a central “tagged” particle. Figure 1 shows $P(r)$ for hard spheres and for a HCYF with $z=7$ at high densities: the influence of a deep attractive potential is rather manifest in the contact region up to $r \approx 1.5\sigma$. A radial integral of the histogram readily yields the mean NN separation l . We find that $n_{\text{NN}} \approx 14.5$ at freezing densities, an estimate that is definitely larger than the coordination number n_c of a simple dense fluid or, even, of a hard-core fluid at closest packing ($n_c = 12$). This apparently paradoxical result is the subtle outcome of a geometrical “marginality” problem whose origin can be explained by resorting, for simplicity, to the crystalline structure of such fluids. As is well known, the Voronoi cell relative to a perfect FCC lattice is a rhombic dodecahedron (in this case the Voronoi cell is nothing but the Wigner–Seitz cell). Six vertices of the dodecahedron are each equidistant between the chosen central particle and one of the six particles forming its second coordination shell. However, it is easy to realize that even a minute perturbation of this structure—as can be induced, for instance, by a thermal fluctuation—discloses a few extra small faces on the surface of the cell (three, on average) which are orthogonal to the lines joining the central particle with particles lying within the second coordination

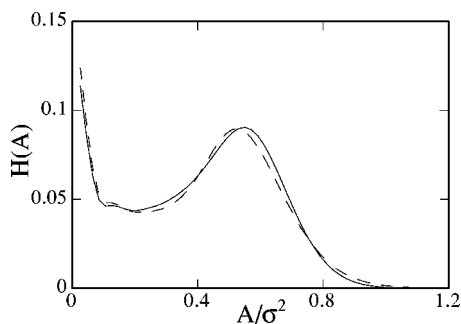


FIG. 2. Frequency of the surface areas of the Voronoi-cell faces (legend as for Fig. 1).

shell. As a result, such particles are classified nearest neighbors in the sense of Voronoi even if their separation from the central particle is larger, on average, than that of the other more “internal” neighbors belonging to the first coordination shell. This somewhat anomalous situation can also be visualized through the histogram shown in Fig. 2, representing the average distribution of the surface areas of the Voronoi polygons: the presence of a subsidiary peak centered at zero is the fingerprint of the existence of such marginally neighboring particles.

Figure 3 shows the mean NN separation l , plotted as a function of the density, for hard spheres and for a HCYF with two different decay ranges of the potential ($z=3.9,7$) and at different temperatures as well. The data can be fitted with a simple $c \cdot \rho^{-1/3}$ law, where $c \approx 1.22$. The value obtained for the constant c is very close to $\sigma \rho_{\text{CP}}^{1/3} = 1.12 \dots$, where $\rho_{\text{CP}} = 2^{1/2} \sigma^{-3}$ is the HS density at closest packing. In fact, one would expect to recover $l = \sigma$ as a lower-bound value for a close-packed assembly of spherical hard-core particles. The tiny overestimate of the constant c that was obtained through the fit, with the resulting moderate but systematic stretching of the average NN distances, is the outcome of the marginality problem discussed above, i.e., of the average inclusion of three more distant second-shell neighbors in the calculation of l . As a result, on approaching close packing, the mean NN separation calculated according to Voronoi no longer saturates at σ but, rather, at $[(12+3 \cdot 2^{1/2})/15]\sigma \approx 1.08\sigma$, a value that is consistent with the fit of

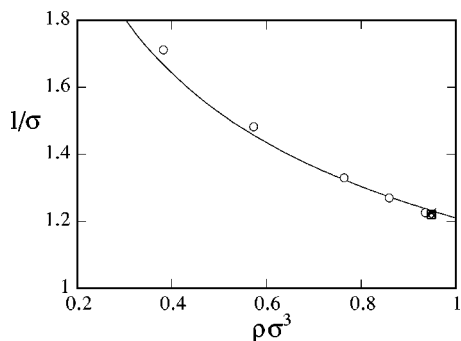


FIG. 3. Nearest-neighbor distances estimated as a function of the reduced density for hard spheres through the Voronoi construction (open circles). Some data points relative to the HCYF for $\rho\sigma^3=0.95$ and for different values of z and T^* are also shown but are hardly resolved on the scale of the plot. The data are fitted to the curve $l(\rho) = 1.22\sigma \cdot \rho^{-1/3}$ (continuous line).

TABLE I. Thermodynamic states where the RMPE vanishes for the model potentials investigated.

Model	z	T^*	$\rho_0\sigma^3$	$\rho_f\sigma^3$
HS			0.95	0.94 ^a
LJ		0.75	0.86	0.87 ^b
LJ		1.15	0.96	0.94 ^b
LJ		2.00	1.04	1.04 ^b
LJ		2.74	1.11	1.11 ^b
HCYF	3.9	0.60	0.95	0.85 ^c
HCYF	3.9	0.70	0.95	0.90 ^c
HCYF	3.9	2.00	0.95	0.95 ^c
HCYF	7.0	0.50	0.95	0.70 ^c
HCYF	7.0	1.00	0.95	0.94 ^c

^aReferences 22 and 23.

^bReference 19.

^cVisual estimates from Ref. 14.

the data presented in Fig. 2. In any case, given that only the ratios of the average NN separations are needed in Eq. (7) for the scaling of the interparticle distances, the dependence of l on the density can be safely estimated as $\rho^{-1/3}$ (as already done in Ref. 1), regardless of the value assigned to the constant c . This approximation turns out to be quite reliable also for the LJ potential, as indirectly witnessed by the comparison of scaled RDF's that is presented in the forthcoming section.

IV. RESULTS

The thermodynamic states where we tested the scaling criterion for the three model fluids investigated are listed in Table I. We also included—for each fluid and temperature—the values of the freezing densities ρ_f , independently obtained by other authors with numerical simulation methods, for a comparison with the “intrinsic” ordering threshold ρ_0 that is associated with the vanishing of the RMPE.

The scaling procedure illustrated in the preceding section was originally tested for the LJ fluid versus hard spheres.¹ We have now extended the comparison to include four different thermodynamic states along the zero-RMPE locus. It is well known that the indications given by the entropy criterion are pretty consistent, also on the quantitative side, with the thermodynamically established freezing threshold of the LJ fluid and bare hard spheres.^{3,4} Figure 4 shows the corresponding RDF's: it is rather manifest that, within the numerical resolution of the calculation, the amplitudes of the oscillations—beyond the first peak—do actually coincide. This is true for both the LJ fluid along the zero-RMPE locus as well as for hard spheres at the one single density where the RMPE happens to vanish. Furthermore, after scaling the interparticle distances according to the criterion exposed in the preceding section, all of the RDF's are found to collapse onto a unique profile. We have tried to ascertain whether the merging of the LJ RDF's onto a common profile might be considered as accidental by checking the sensitivity of the RDF's to temperature changes at a fixed density. Figure 5 shows such a comparison for $\rho\sigma^3=0.86$ and 0.96. The temperatures at which we sampled the fluid are the same as those sorted out at different densities by the zero-RMPE constraint. As can be appreciated from Fig. 5,

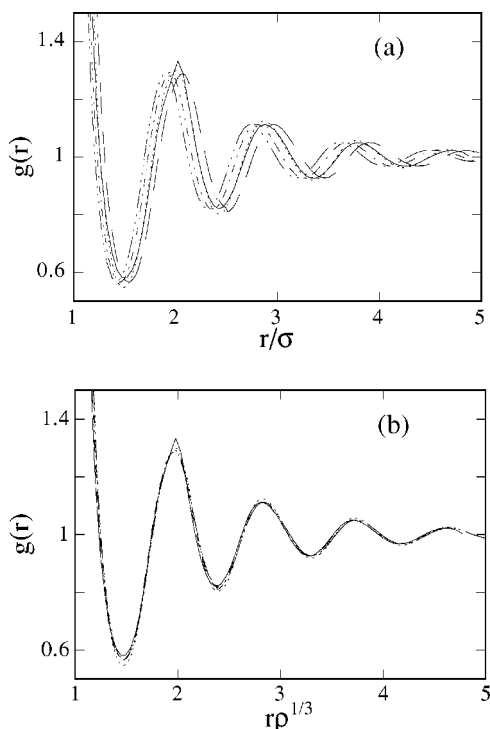


FIG. 4. Radial distribution functions of hard spheres and of a Lennard-Jones fluid in thermodynamic states characterized by the vanishing of the residual multiparticle entropy (see Table I). Hard spheres: continuous line; Lennard-Jones: dashed line ($T^*=0.75$), dotted line ($T^*=1.15$), dot-dashed line ($T^*=2$), dot-dot-dashed line ($T^*=2.74$). The curves reported in the lower part (b) of the figure are the same as in (a) but for the use of scaled distances $r \cdot \rho^{1/3}$.

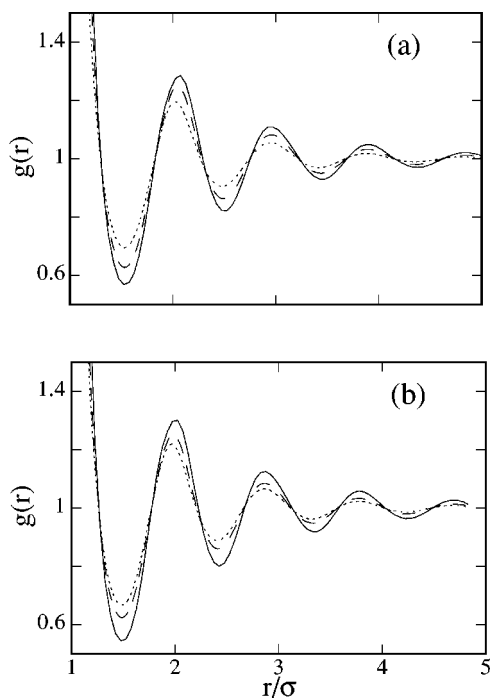


FIG. 5. A check of the sensitivity of the radial distribution function of the Lennard-Jones fluid to temperature changes at a fixed density: (a) $\rho\sigma^3 = 0.86$: continuous line ($T^*=0.75$), dashed line ($T^*=1.15$), dotted line ($T^*=2$). (b) $\rho\sigma^3 = 0.96$: continuous line ($T^*=1.15$), dashed line ($T^*=2$), dotted line ($T^*=2.74$).

the amplitudes of the RDF's now differ in a significant way. Hence, it appears that the claimed correspondence is correctly assured only if one compares the properties of the fluid relative to thermodynamic states where $\Delta s(\rho, T) = 0$, a condition which, in general, implies different densities at different temperatures.

In order to check the generality of Eq. (6), we have also considered another standard model fluid, i.e., the HCYF. As formerly anticipated, we investigated the properties of this model for two values of the decay parameter, $z = 3.9$ and 7 , respectively, corresponding to a progressively shorter and shorter range of the attractive tail. According to numerical simulation, for $z = 3.9$, the HCYF still has a liquid phase which, however, becomes metastable with respect to sublimation for $z \approx 7$.¹⁴ Other authors have already used the entropy criterion in order to predict the freezing point of the HCYF.^{15–18} The most refined integral-equation theories (MHNC, SCOZA) reveal a scarce sensitivity of the zero-RMPE density threshold with respect to temperature shifts.^{16,17} As a result, the corresponding locus in the ρ, T diagram apparently fails to account for the “softening” of the freezing line that is registered by numerical simulation at intermediate densities when the range of the potential becomes very short. This shortcoming is even accentuated by the alternative use of the criterion formerly proposed by Hansen and Verlet (HV) for estimating the freezing point of the fluid.¹⁹ However, the numerical implementation of the condition $\Delta s(\rho, T) = 0$ with Gibbs ensemble Monte Carlo data shows that the disappearance of the stable liquid phase would still occur for $z \approx 13$.¹⁸ The present results, which are based on a numerical simulation of larger samples, are consistent—within a common range of the parameters—with those obtained in Ref. 18. In fact, Table I shows that $\rho_0(T)$ sticks, for both values of the decay parameter z , at the HS value over a wide temperature range. Actually, for $z = 7$, we observed a modest bending of the zero-RMPE line towards decreasing densities for deep metastable states only, i.e., at temperatures lower than 0.5 . Of course, the failure of the entropy-based criterion, as well as of the HV recipe, in modeling the shape of the transition line for very short-ranged potentials may be the outcome of an intrinsic deficiency of both criteria which becomes particularly evident in the case of such anomalous, almost adhesive potentials. However, it may also be an indirect indication of the fact that the thermodynamic gas-solid transition which occurs in this peculiar regime is conditioned by increasing stronger “energy” effects, at variance with the underlying structural modifications that are quite sensitively detected by the entropy criterion at higher densities. These structural effects, which are associated with the existence of a metastable liquid phase, seem to be altogether important in “assisting” the kinetics of the nucleation of a solid phase.²⁰

Figure 6 shows the RDF's of the HCYF. In passing, we recall that the small hump in the second maximum (slightly more prominent than for bare hard spheres) is a short-distance effect whose appearance (for increasing densities) signals the incoming freezing transition.²¹ The RDF's do substantially overlap for $z = 3.9$. A tiny, but systematic, shift towards smaller distances can be observed only at low tem-

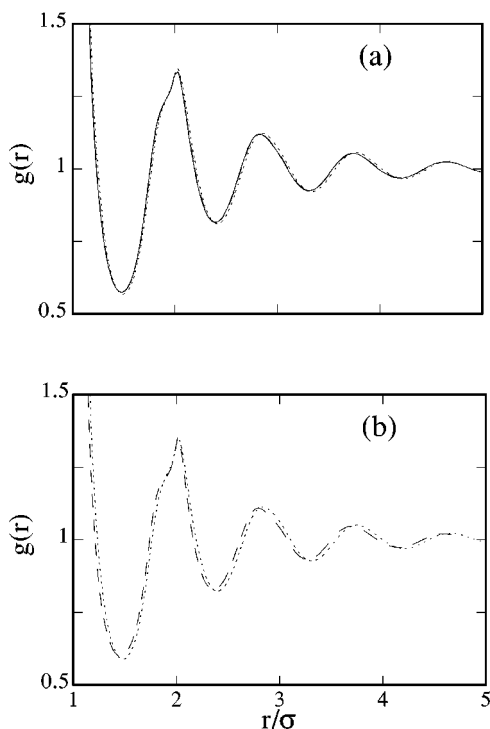


FIG. 6. Radial distribution functions of the HCYF in thermodynamic states characterized by the vanishing of the residual multiparticle entropy (see Table I). (a) HCYF with $z=3.9$: continuous line ($T^*=0.60$), dashed line ($T^*=0.70$), dotted line ($T^*=2$). (b) HCYF with $z=7$: dashed line ($T^*=0.50$), dotted line ($T^*=1.00$).

peratures. Such a relative shift is hardly perceivable for $z=3.9$ but becomes more visible for $z=7$. This effect is clearly originated by the increased cohesion of the fluid at low temperatures, the expected consequence of a rather deep and short-ranged attractive potential. As such, this shift cannot be accounted for by the scaling procedure presented in Sec. III which rests upon a definition of the NN distance which does not significantly depend upon the temperature of the fluid (see Fig. 3). However, what seems lacking in this case is a finer definition of such a distance. The straight definition resulting from the Voronoi construction does not seem completely appropriate in the case of such unconventional potentials, in that it fails to monitor the small but systematic lowering of the relative interparticle distances that is registered upon decreasing the temperature of the fluid at a given density. Such a failure is likely due to the “coarsening” of the currently used distance that is produced by the inclusion of relatively far particles (with respect to the central one), as discussed in detail at the end of the preceding section. In order to check whether this is the case, we considered the following modified definition of the average NN distance:

$$l_w \equiv \left\langle \sum_{\text{NN}} w_i \cdot R_i \right\rangle, \quad (9)$$

where R_i yields the relative distance of the i th NN particle from a given reference one, and w_i is the ratio of the surface area of the associated polygonal face to the total surface area of the Voronoi polyhedron constructed around the central particle. As usual, an averaging is then performed over all

TABLE II. Average nearest-neighbor distances in a HCYF for $z=7$ calculated through the Voronoi construction (see text). The value for $T^*=\infty$ refers to hard spheres with no attraction.

T^*	l	l_w
0.5	1.225	1.116
1.0	1.222	1.120
∞	1.227	1.127

the particles of the fluid and over the MC configurations. The rationale behind this new definition is obviously that the factor w_i progressively reduces the relative weight of the furthest particles in the evaluation of the average NN distance: in fact, the further the neighbor, the smaller the area of the associated polygon. The two quantities, l and l_w , are compared in Table II for the HCYF with $z=7$: The data show that, at variance with the original definition, the weighted distance l_w does depend on the temperature in a weak but systematic way, actually decreasing with T along an isochore, as one would expect on an intuitive basis. Using l_w as the reference quantity, when scaling interparticle distances, almost completely removes the relative shift observed at different temperatures between the RDF's of the fluid (see Fig. 7).

Summing up, the overall evidence on the HCYF appears to be consistent with that discussed for the LJ fluid, while definitely being less stringent, also as a result of the fact that the RDF's singled out by the zero-RMPE constraint refer to the same density. In fact, the amplitudes of the medium-range oscillations coincide, independently of the temperature and of the value of the decay parameter z . However, it is also true that the density profile of the HCYF turns out to be almost insensitive to temperature changes for high enough densities ($\rho\sigma^3 > 0.7$).

V. DISCUSSION AND CONCLUDING REMARKS

As a result of the scaling relation illustrated for fluids with vanishing RMPE by Eqs. (6), (7), and (8), the RDF can be split, at least for the model potentials investigated so far, into the sum of a short-range interaction-dependent part

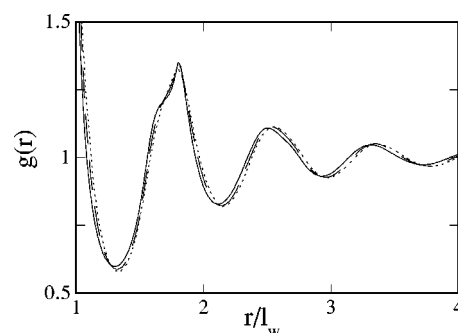


FIG. 7. Radial distribution functions of hard spheres and of the HCYF with $z=7$ in thermodynamic states characterized by the vanishing of the residual multiparticle entropy (see Table I): the relative distances r have all been referred to the area-weighted nearest-neighbor distance l_w . Hard spheres: continuous line; HCYF: dashed line ($T^*=0.50$), dotted line ($T^*=1.00$).

$G_\alpha(r)$ and a seemingly “universal” long-range part $\tilde{g}_\alpha(r)$. Correspondingly, the associated contribution to the total structure factor of the fluid can be written as

$$\begin{aligned}\tilde{S}_\alpha(q) &= 1 + \rho_\alpha \int e^{-i\mathbf{q}\cdot\mathbf{r}} (\tilde{g}_\alpha(r) - 1) d\mathbf{r} \\ &= 1 + \rho_\beta \int e^{-i(\mathbf{q}/\gamma)\cdot\mathbf{r}} (\tilde{g}_\beta(r) - 1) d\mathbf{r} \\ &= \tilde{S}_\beta(q/\gamma),\end{aligned}\quad (10)$$

where the subscripts α , β identify specific model fluids. Hence, apart from minor effects associated with the temperature dependence of the average NN distance, it follows

$$\tilde{S}_\alpha(q\rho_\alpha^{1/3}) \approx \tilde{S}_\beta(q\rho_\beta^{1/3}).\quad (11)$$

As is well known, the long-range oscillations of the RDF contribute in a preponderant way to model the shape of the structure factor of the fluid, $S(q)$, in the region of the first peak. In this respect, having noted that the ordering condition associated with the vanishing of the RMPE is the fingerprint—in the fluid phase—of the freezing of a 3D fluid, the simple scaling law stated by Eq. (11) for the “partial” structure factor $\tilde{S}(q)$ shows up as a complementary but self-contained version of the HV criterion. In fact, this latter criterion rests upon an “external” phenomenological observation relative to the height (~ 2.85) of the first maximum of $S(q)$ at freezing. However, apart from a finer dependence of this value on the nature of the potential, it also turns out that such a value is different in different spatial dimensions, even for the same model fluid. Instead, the overall profile (not only the height) of the partial structure factor $\tilde{S}(q)$ is found to scale uniformly both in 2D as well as in 3D along the thermodynamic locus characterized by the vanishing of the RMPE. From this perspective, the entropy criterion yields a more general statement than that following from the HV rule. However, both criteria identify an intrinsic structural condition of the fluid which, in the enlightening perspective of-

ferred by the multiparticle correlation expansion of the statistical entropy, reveals itself as the microscopic backstage of the incoming transition of the fluid into a more ordered state.

ACKNOWLEDGMENT

The authors wish to thank Dr. D. Costa for providing a copy of the simulation code of a HCYP and for useful discussions.

- ¹F. Saija, S. Prestipino, and P. V. Giaquinta, *J. Chem. Phys.* **113**, 2806 (2000).
- ²R. E. Nettleton and M. S. Green, *J. Chem. Phys.* **29**, 1365 (1958).
- ³P. V. Giaquinta and G. Giunta, *Physica A* **187**, 145 (1992).
- ⁴P. V. Giaquinta, G. Giunta, and S. Prestipino Giarritta, *Phys. Rev. A* **45**, R6966 (1992).
- ⁵C. Caccamo, P. V. Giaquinta, and G. Giunta, *J. Phys.: Condens. Matter* **5**, B75 (1993).
- ⁶F. Saija, P. V. Giaquinta, G. Giunta, and S. Prestipino Giarritta, *J. Phys.: Condens. Matter* **6**, 9853 (1994); F. Saija and P. V. Giaquinta, *ibid.* **8**, 8137 (1996).
- ⁷P. V. Giaquinta, G. Giunta, and G. Malescio, *Physica A* **250**, 91 (1998).
- ⁸F. Saija, G. Pastore, and P. V. Giaquinta, *J. Phys. Chem.* **102**, 10368 (1998).
- ⁹D. Costa, F. Saija, and P. V. Giaquinta, *Chem. Phys. Lett.* **282**, 86 (1998); *ibid.* **299**, 252 (1999).
- ¹⁰S. Prestipino and P. V. Giaquinta, *J. Stat. Phys.* **96**, 135 (1999); *ibid.* **98**, 507 (2000).
- ¹¹M. G. Donato, S. Prestipino, and P. V. Giaquinta, *Eur. Phys. J. B* **11**, 621 (1999).
- ¹²J.-P. Hansen and D. Schiff, *Mol. Phys.* **25**, 1281 (1973).
- ¹³See, for instance, C. A. Rogers, *Packing and Covering* (Cambridge University Press, Cambridge, 1964).
- ¹⁴M. H. J. Hagen and D. Frenkel, *J. Chem. Phys.* **101**, 4093 (1994).
- ¹⁵C. Caccamo, D. Costa, and G. Pellicane, *J. Chem. Phys.* **109**, 4498 (1998).
- ¹⁶C. Caccamo, G. Pellicane, D. Costa, D. Pini, and G. Stell, *Phys. Rev. E* **60**, 5533 (1999).
- ¹⁷C. Caccamo, G. Pellicane, and D. Costa, *J. Phys.: Condens. Matter* **12**, A437 (2000).
- ¹⁸K. P. Shukla, *J. Chem. Phys.* **112**, 10358 (2000).
- ¹⁹J.-P. Hansen and L. Verlet, *Phys. Rev.* **184**, 151 (1969).
- ²⁰P. R. ten Wolde and D. Frenkel, *Science* **277**, 1975 (1997).
- ²¹T. M. Truskett, S. Torquato, S. Sastry, P. G. Debenedetti, and P. H. Stillinger, *Phys. Rev. E* **58**, 3083 (1998).
- ²²W. G. Hoover and F. H. Ree, *J. Chem. Phys.* **49**, 3609 (1968).
- ²³L. V. Woodcock, *Nature (London)* **385**, 141 (1997).